Thesis Report

On

EFFECT OF FINITE ELEMENT MESH ORIENTATION ON THE SOLUTION ACCURACY OF TORSIONAL PROBLEMS

Submitted in the partial fulfillment of requirement for the award of the degree of

Master of Engineering

IN

MECHANICAL

(CAD/CAM and ROBOTICS)

Submitted by

YATHESHTH ANAND
Roll No. : 8048125

Under the guidance of

Mr. J.S.SAINI
Lecturer
T.I.E.T, Patiala

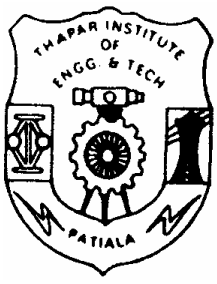

Department of Mechanical Engineering
THAPAR INSTITUTE OF ENGINEERING AND TECHNOLOGY
(DEEMED UNIVERSITY)
PATIALA (PUNJAB)-147004

Acknowledgement

I express my sincere gratitude to my guide**, Mr. J.S.SAINI** Lecturer, Mechanical Engg. Department at Thapar Institute of Engineering & Technology, for his valuable guidance, proper advice, painstaking and constant encouragement during the course or my work on this seminar.

I also feel very much obliged to **Dr. S.K MOHAPATRA,** Professor & Head, Department of Mechanical Engg. for his encouragement and inspiration for execution of the seminar work.

I am deeply indebted to my parents for their inspiration and ever encouraging moral support, which enabled me to pursue my studies.

I am also very thankful to the entire faculty and staff members of Mechanical engineering Department for their direct–indirect help and cooperation.

Dated:

YATHESHTH ANAND

(ROLL NO. 8048125)

CERTIFICATE

This is to certify that the Thesis report entitled**, "EFFECT OF FINITE ELEMENT MESH ORIENTATION ON THE SOLUTION ACCURACY OF TORSIONAL PROBLEMS"** submitted by **Mr. YATHESHTH ANAND** in the partial fulfillment of the requirement for the award of the degree of **Master of Engineering in Mechanical (CAD/CAM and ROBOTICS) Engineering** to **Thapar Institute of Engineering and Technology (Deemed University), Patiala,** is a record of candidate's own work carried out by him under my supervision and guidance. The matter embodied in this report has not been submitted in part or full to any other university or institute for the award of any degree.

(Mr. J.S.SAINI)
Lecturer, Mechanical Engineering Department.
Thapar Institute of Engg. &Technology,Patiala

Countersigned by:

Dr. S.K. MOHAPATRA
Prof. & Head, MED.
THAPAR INSTITUTE OF ENGG. &TECH.
PATIALA-147004(PUNJAB)

Dr. T.P. SINGH
Dean, Academic Affairs
THAPAR INSTITUTE OF ENGG. &TECH.
PATIALA-147004(PUNJAB)

Dated:

ABSTRACT

In the mechanical systems there are numerous applications of torque, which results in the failure of a component due to shear stress if not properly designed. It becomes essential to examine the amount of torque, a component can sustain without failure.

Now, Finite Element Method which has increasingly becoming an integral tool for CAD due to the ongoing revolution in computer field is used for the analysis of torque by number of researchers.

Finite Element Mesh orientation has an effect on the accuracy of the solution. The present work describes the effect of triangular Finite Element Mesh orientation with regards to torsion.

LIST OF FIGURES

CHAPTER 1

CHAPTER 3

CHAPTER 4

INDEX

CHAPTER-3

CHAPTER-4

CHAPTER-5

INTRODUCTION CHAPTER-1

In the present work, the effect of mesh orientation on the beam member when subjected to torsion is analyzed, using FEM. Here it becomes necessary to know the related terms.

1.1 TORSION

Torsion refers to the twisting of a structural member when it is loaded by couples that produce rotation about its longitudinal axis. These couples that produce twisting of bars are called torques, twisting couples, or twisting moments. When a uniform prismatic bar is subjected to a torque so that bending is zero then every section of the bar is subjected to a state of pure shear. The moment of resistance developed by the shear stresses being everywhere equal to the magnitude, and opposite in sense, to the applied torque.

1.1.1 TORSION OF CIRCULAR SHAFTS

A circular cylindrical shaft is said to be subjected to pure torsion when the torsion is caused by a coupling, so that the axis of the applied couple coincides with the axis of the shaft. In such a case the state of stress at any point in the cross-section of the shaft is one of pure shear, and the strain is such that one cross-section of the shaft moves relative to another. Some assumptions in torsion of circular shafts:

1. That the material of the bar is homogenous i.e. perfectly elastic and obeys Hook's Law.
2. The stress doesn't exceed the limit of proportionality
3. Cross-sections rotate as if rigid, i.e. every diameter rotates through the same angle.
4. Circular sections remain circular.

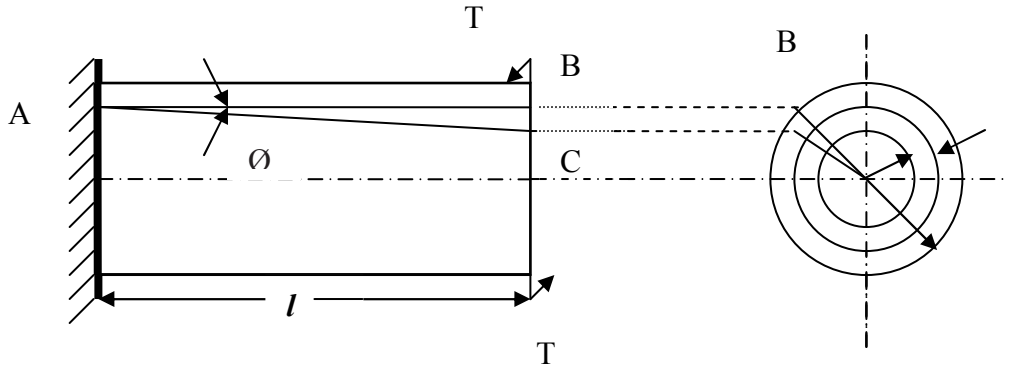

Fig.1.1 Pictorial View of a Shaft in Torsion

Consider a circular shaft of length l and diameter d subject to a couple T as shown in the Fig. 1.1 at one end, the other end is rigidly fixed or held by a balancing couple of equal amount. A line AB on the surface of the shaft, which is parallel to the axis before straining, takes up the form of a helix AC after straining. Let ϕ be the angle of shear strain on the surface. Then,

$$BC = l\phi$$

or $$\phi = \frac{BC}{l}$$

But $$\phi = \frac{\tau}{G} \quad \ldots\ldots\ldots\ldots\ldots\ldots\ldots\ldots\ldots\ldots\ldots\ldots\ldots\ldots\ldots\ldots \quad (1.1)$$

where τ = Shear stress in shaft

G = Modulus of rigidity

$\therefore$ $$\tau = \phi G$$

Now $$BC = \frac{d}{2}.\theta$$

where θ = Angle of twist

$$\tau = \frac{d}{2}.\frac{\theta}{l}.G = \left(\frac{G\theta}{l}\right).\frac{d}{2} = \text{k. r} \ldots\ldots\ldots\ldots\ldots\ldots\ldots\ldots\ldots\ldots\ldots\ldots\ldots\ldots\ldots\ldots \quad (1.2)$$

where $k = \frac{G\theta}{l}$ is constant for a given shaft

$r = \frac{d}{2}$ is the shaft radius

Thus the shear stress in the shaft is proportional to the radius of the shaft. At any radius x, $\frac{\tau_x}{\tau} = \frac{x}{r}$

or $\tau x = \frac{x}{r} . \tau$

Also $\frac{\tau}{r} = \frac{G\theta}{l}$

Now consider an elementary ring of the shaft at a radius x and of thickness dx as shown in the Fig. 1.1 the shear stress in the ring is τ_x.

Total force on the ring = Area of the ring $\times \tau_x = 2\pi x dx \times \tau_x$

Moment of this force about the axis of the shaft

$$= 2\pi x dx \times \tau_x \times x = 2\pi x 2dx. \tau_x$$

$$= 2\pi x 2dx \frac{x}{r} \tau = 2\pi x 3\ dx \frac{\tau}{r}$$

Total resisting moment of the shaft cross-section is

$$= 2\pi \frac{\tau}{r} \int_0^r x^3\ dx = 2\pi \frac{\tau}{r} . \left| \frac{x^4}{4} \right|_0^r$$

$$= 2\pi \frac{\tau}{r} . \frac{r^4}{4} = \frac{\pi r^3}{2} . \tau$$

But total resisting moment of the section = Applied torque T

$$T = \frac{\pi r^3}{2} \tau = \frac{\pi d^3}{16} . \tau = \frac{\tau}{(d/2)} . \left(\frac{\pi d^4}{32} \right) = \left(\frac{\tau}{(d/2)} \right) . J \quad \text{..... (1.3)}$$

where $J = \frac{\pi d^4}{32}$ is the polar moment of inertia of the shaft cross-section

$$\therefore \quad \frac{T}{J} = \frac{\tau}{r} = \frac{G\theta}{l} \quad \text{..... (1.4)}$$

This is the torsion formula for shafts of circular cross-section.

1.2 FINITE ELEMENT METHOD

The term finite element was first coined and used by Clough in 1960. Since then it has become a powerful tool for the numerical solution of a wide range of engineering problems. Applications range from deformation and stress analysis of automotive, aircraft, building and bridge structures to field analysis of heat flux, fluid flows, magnetic flow, seepage, and other flow problems.

1.2.1 HISTORIC BACKGROUND

Basically, the very basic idea of the finite element originated from advances in aircraft structural analysis. Hrenikoff presented a solution of elasticity problems using the "frame work problems". Courant's paper, which used piecewise polynomial interpolation over triangular sub regions to model torsion problems, appeared in 1943. Turner, et al. derived stiffness matrices for truss, beam and other problems and presented their findings in 1956.A book by Argyris in1955 on energy theorems and matrix methods laid a foundation for further developments in finite element studies. The first book on finite elements by Zienkiewicz and Chung was published in 1967.

1.2.2 TECHNIQUE

The finite element method is a numerical analysis technique used by engineers, scientists, and mathematicians to obtain solutions to the differential equations that describe, or approximately describe a wide variety of physical (and non-physical) problems. Physical problems range in diversity from solid, fluid and soil mechanics, to electromagnetism or dynamics.

The underlying premise of the method states that a complicated domain can be sub-divided into a series of smaller regions in which the differential equations are approximately solved. By assembling the set of equations for each region, the behavior over the entire problem domain is determined.

Each region is referred to as an element and the process of subdividing a domain into a finite number of elements is referred to as discretization. Elements are connected at specific points, called nodes, and the assembly process requires that the solution be continuous along common boundaries of adjacent elements.

A finite element analysis involves three stages of activity:

- Preprocessing
- Processing
- Post processing

- PRE-PROCESSING

  Pre-processing involves the preparation of data, such as nodal coordinates, connectivity, boundary conditions, and loading and material information.

- PROCESSING

  The processing stage involves mesh generation, stiffness matrix generation, its modification, and solution of equations, resulting in the evaluation of nodal variables. Other derived quantities, such as gradients or stresses may be evaluated in this stage.

- POST-PROCESSING

  The post-processing stage deals with the preparation of the results. Typically, the deformed configuration, mode shapes, temperature, and stress distribution are computed and displayed at this stage.

A complete finite element analysis is a logical interaction of these three stages.

➢ DISCRETIZATION USING FINITE ELEMENTS

Using the finite element method, the solution domain is discretized into smaller regions called elements, and the solution is determined in terms of discrete values of some primary field variables φ (e.g. displacements in x, y z directions) at the nodes. The number of unknown primary field variables at a node is the degree of freedom at that

node. For example, the discretized domain comprised of triangular shaped elements is shown below left: In this example each node has one degree of freedom.

The governing differential equation is now applied to the domain of a single element. At the element level, the solution to the governing equation is replaced by a continuous function approximating the distribution of φ over the element domain De, expressed in terms of the unknown nodal values $\varphi 1$, $\varphi 2$, *and* $\varphi 3$ of the solution φ.

A system of equations in terms of $\varphi 1$, $\varphi 2$, and $\varphi 3$ can then be formulated for the element.

Once the element equations have been determined, the elements are assembled to form the entire domain D. The solution $\varphi(x,y)$ to the problem becomes a piecewise approximation, expressed in terms of the nodal values of φ. A system of linear algebraic equations results from the assembly procedure. For practical engineering problems, it is not uncommon for the size of the system of equations to be in the thousands, making a digital computer a necessary tool for finding the solution.

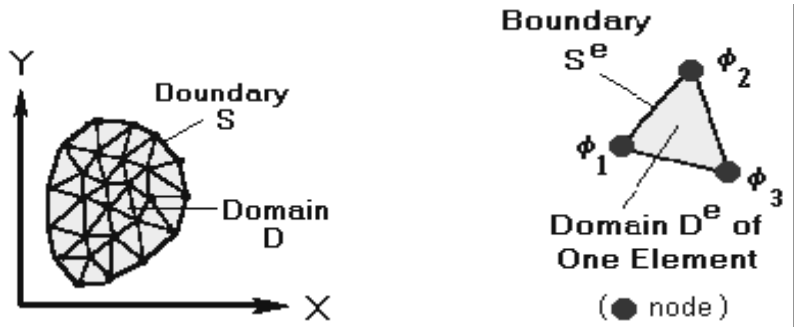

Fig. 1.2 Discretization Using Finite Elements

1.2.3 FEM PROCEDURE

The procedure of FEM is based on following steps:

1. Representation of continuous structure as a collection of grid points connected by discrete elements.
2. Formulation of element stiffness matrix from element properties i.e. geometry and material properties.

3. Assembly of global stiffness matrix from element stiffness matrix.
4. Boundary conditions are applied.
5. Generation of load vector.
6. A series of simultaneous equations are then solved to find the unknown parameters.

1.2.4 APPLICATIONS OF FINITE ELEMENT ANALYSIS

The most utilization of FEM is in finding stresses and strains caused by loading conditions on a part. Other applications of FEM include:

- Static stress-strain problems
- Non-linear problems
- Heat transfer problems
- Modal analysis
- Dynamic analysis
- Electricity and magnetism problems
- Flow problems
- Acoustic problems and other engineering problems in various fields

1.3 ELEMENT SHAPES

The process of discretizing or subdividing a continuum is an exercise of engineering judgment. The first decision the engineer must make is to the shape or configuration of the basic element to be used in the analysis. This choice depends upon the geometry of the body or structure and upon the number of independent space coordinates (e.g. x, y, or z) necessary to describe the problem. A finite element usually has a simple one-, two-, or three-dimensional configuration. The boundaries of elements are often straight lines, although for problems that can be best represented in curvilinear coordinates, it is advantageous for the element shapes to be similarly defined.

1.3.1 ONE-DIMENSIONAL ELEMENTS

When the geometry, material properties, and such dependent variables as a displacement can all be expressed in terms of one independent space coordinates, a one-

dimensional element is appropriate. This coordinate is measured along the axis of the element. This type of element is used for structures that can be idealized by line drawings, such as the frame. Frame analysis is done when one-dimensional elements are considered, because a distinguishing characteristic of the finite element method is that the elements themselves are continuous two- or three-dimensional bodies. However, a finite element approach to the analysis of beams and framed structures produces some useful insights, particularly when the geometry and properties of the structure vary continuously or discontinuously with the axial coordinates. In addition, one-dimensional problems are a simple but useful tool for developing our understanding of the finite element method.

A one-dimensional element may be represented by a straight line whose ends are nodal points. These nodal points, numbered 1 and 2 in the Fig.1.3, are called external nodes because they represent connecting points to the adjacent elements. Some applications may require additional nodal points, such as node 3 in Fig.1.3. Because no connection to other elements occurs at this intermediate node, it is called an internal node.

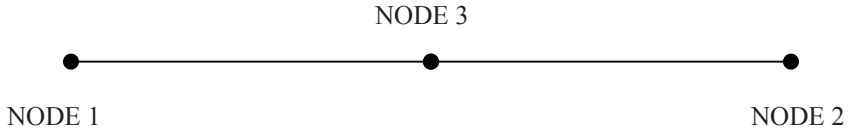

Fig. 1.3 One-dimensional element

1.3.2 TWO DIMENSIONAL ELEMENTS

The simplest element for two-dimensional problems is a triangle as shown in Fig. 1.4(a). There are two possible types of external nodes for triangular elements. The corner nodes indicated by 1, 2, and 3 in Fig. 1.4(a) are called primary external nodes.

When additional nodes occur on the sides of the element, like nodes 4, 5, and 6 in Fig.1.4 (a), these are referred as secondary external nodes. This distinction is necessary because the secondary nodes may have fewer displacements of interest than the corner nodes. Finally, internal nodes, such as node 7 in Fig. 1.4(a), are sometimes also used in triangular elements. Other common types to two-dimensional element are the rectangular and quadrilateral shapes, Fig. 1.4(b) and Fig. 1.4(c). The former can be considered a

specialization of the latter. Although practically two-dimensional continuum can be represented by an assemblage of triangles, there are certain problems in which quadrilateral elements are advantageous. Instead of directly using quadrilateral elements, it is possible to construct such shapes from two or four triangular elements, as shown in Fig. 1.4(d) and Fig. 1.4(e). In addition to the primary external nodes shown in Fig.1.4(b) through Fig. 1.4(e), each of the quadrilateral elements may also have secondary external nodes and one or more internal nodes.

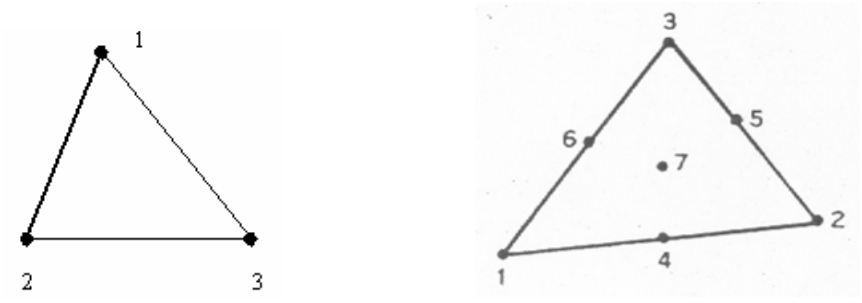

(a) Triangular element

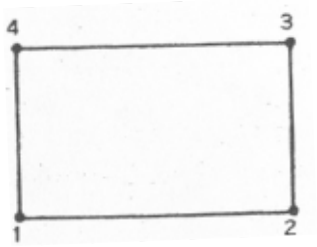

(b) Rectangular element

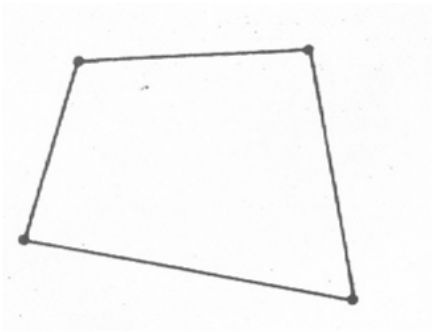

(c) Quadrilateral element

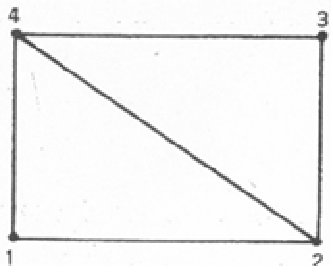

(d) Quadrilateral formed by two triangles

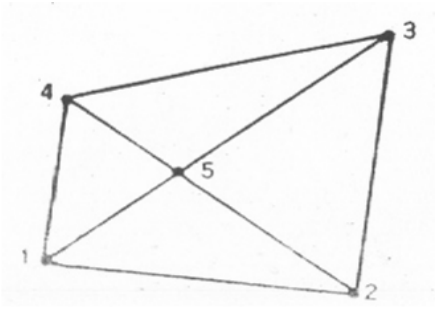

(e) Quadrilateral formed by four triangles

Fig. 1.4 Two-dimensional element

1.3.3 THREE-DIMENSIONAL ELEMENTS

Corresponding to the triangle, the tetrahedron shown in Fig. 1.5(b) is the basic finite element for three-dimensional problems. A tetrahedron has four primary external nodes. Three-dimensional elements with eight primary external nodes are either in the form of a general hexahedron, Fig. 1.5(c), or a rectangular prism, Fig. 1.5(a), which is the specialization of a hexahedron. If necessary, secondary external nodes or internal nodes for each of these elements can be introduced.

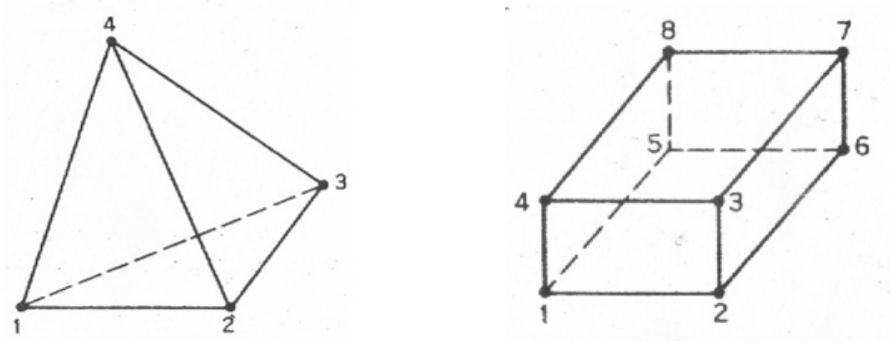

(a) Tetrahedron (b) Rectangular Prism

Fig. 1.5 Three-dimensional elements

1.4 MESH ORIENTATION

In the finite element analysis the domain is discretised into smaller elements, which can be a line, square, triangular or tetrahedron etc. Based on whether the problem is of 1D, 2D or 3D. In some cases a combination of elements is also used based on the type of the geometry of the domain.

Despite the fact that the finite element mesh generation has been developing over several decades. Now, a variety of real life engineering problems imposes additional requirements on the existing mesh generation technologies. For example, mesh orientation zones around, finding the most appropriate placement of the mesh elements so that more accurate and smother results are obtained.

Orientation of mesh doesn't come to play in the case of square elements as their geometry remains unchanged in either of the orientation. But when triangular elements are considered the case changes and here the difference of geometry and connectivity

arises, which can put some effect on the results. Now, as on solving the FEM problem the co-ordinates of the member as per their connectivity are taken and put into the respective formula and the result are obtained. From the Fig. 1.6, it is clear that the new orientation will have no effect on the connectivity of the square element but this would not be the case when triangular element is considered. Here, with the change of the orientation the co-ordinates will change hence the results would vary with the orientation.

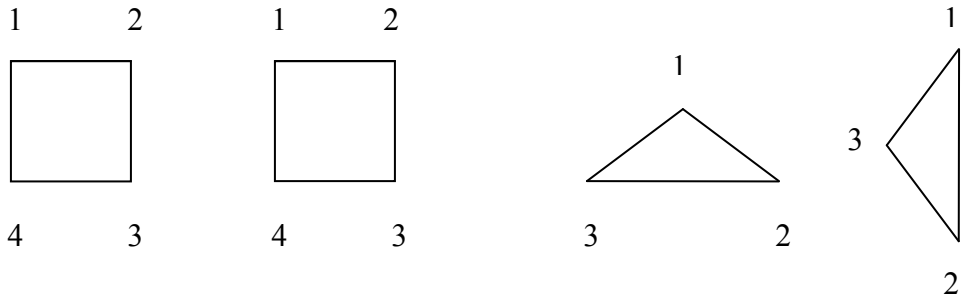

(a) Square element (b) Triangular element

Fig. 1.6 Orientation difference in case of triangular elements

When the geometry is simple then any type of element can be used according to the problem & according to the will of the analyst. But when the domain is irregular or discontinuous then especially triangular elements are used as they can be easily fitted to any shape.

The present work deals with the different orientations for the triangular elements.

This chapter deals with the review of the work done on the topic. Firstly the review is on the torsion related work. Shear plays an important role in the failure of components subjected to torsion. Then the concentration shifts on the review on the use finite element method in the torsional problems. A number of researchers have gone ahead with the problems of torsion in different components and most of them had used finite element method to analyze them. The following paragraph gives an insight of the work done on torsion using finite element method.

2.1 LITERATURE REVIEW

Nouailhas and Cailletaud [1] investigated the macroscopic behavior of single-crystal super alloys under tension-torsion or torsion loadings. Specific tests were performed at room temperature on a tubular specimen equipped with micro strain-gauges for local deformation measurements, using finite element analysis and a comparison of theoretical and experimental results was made.

Mentrasti [2] formulated the static behavior of circular beams with thin walled open closed cross-section. The influence of the different radius of curvature of each element of the cross section was taken into account, assuming the hypothesis of linear elasticity and that the distortion of the cross-section. Topological properties within the scope of *Graph Theory* were considered for the nodal equilibrium and compatibility conditions for both pure and non-uniform torsion were presented. Also the derivation of warping shape function for pure torsion and the equilibrium equations governing non-uniform torsion were done. Some new aspects, relevant to the compatibility of equilibrium equations and the uncoupling conditions between torsion and both normal force and bending, were discussed extensively.

Loughlan and Ata [3] gave a simple engineering theoretical analysis which was able to predict the initial constrained torsion response of a specific class of thin walled

open section carbon fiber composite beams. This procedure accounts for the effect of primary warping constraint only and thus its application is restricted to the behaviour of sections for which primary warping is predominant. The effects of secondary warping through the thickness of the thin walls are precluded in the theoretical approach. A finite element study was done and was compared with the simple engineering theoretical approach for the Z and channel sections.

Hu *et.al* [4] derived the fourth order governing differential equations for thin walled beams with asymmetric cross-sections under coupled bending and torsion. The stiffness matrix and the consistent mass matrix of a thin-walled beam element with an asymmetric cross-section was established by using the homogeneous solutions to the fourth order governing differential equations as interpolation functions between the degrees of freedom at each node of the element. The shear effect and the coupling between bending and torsion were fully taken into account in the finite element method developed.

Morrell *et.al* [5] studied the effect of torsion when applied to one member of a structure formed from two thin walled open members connected at 90°, can result in torsion as well as flexure in the second member, with the magnitude and direction of this torsion and flexure being determined by the type of joint used. The results from a finite element study of structures formed from thin-walled channel sections connected by box, mitre and stiffened mitre joints were presented and an explanation for the behaviour of the different joint types was given. It was shown that for the box joint the warping deformation of the loaded member was the dominant factor in determining the magnitude and direction of the twisting of the second member, whilst this was determined for the stiffened mitre joint primarily by the St Venant rotation deformation of the loaded member. For the unstiffened joint it is shown that the warping and St Venant rotation deformation effects tend to cancel each other out.

Nori *et.al* [6] used the impulse frequency response vibration technique for determining the shear modulus of glass/epoxy, graphite/epoxy and hybrid (glass-

graphite/epoxy) pultruded cylindrical composite rods in torsion. Fibers and matrix distribution in the shell–core regions were examined microscopically and the volume fractions of various constituents were found using the stereo logy point counting technique. Based on the examined cross-section finite element meshes were generated and analyzed for prediction the shear modulus of such composite rods. After this the finite element results and the experimental results were matched and were found to be in close agreement with each other.

Mitsuya *et.al* [7] studied two cantilevers- rectangular and V-shaped using finite element method for the coupling and nonlinear problems arising in the large scale deformation due to vertical and lateral forces. Sensitivity to lateral force is found to decrease with increasing vertical force, until the critical value of zero is reached. Then, the sensitivity becomes negative with further increases in the vertical force. As for the nonlinear effect, the torsional stiffness against the lateral force was found to exhibit soft apring characteristics for a small vertical force, and hard spring characteristics for a larger range. At the point of the transition, the nonlinear effect appears to diminish. It is interesting to note that at the precise point of transition, the coupling effect between the deflection and torsion was also eliminated, which constitutes the optimum condition for simultaneous measurement of the vertical and lateral forces.

Loughlan and Ata [8] gave an analytical procedure for determining the constrained torsional response of a specific class of carbon fiber composite box-beams using the existing theories of torsion appropriate to isotropic construction and were suitably modified to account for the non-isotropic nature of typical carbon fiber composite material. The constrained condition of cantilevered box-beam with torque applied at the free end and the torsion and warping rigidities of the composite box-sections were determined through the use of the appropriate equivalent engineering elastic constants of the individual thin composite walls. Comparison between theoretical and the finite element solutions were given.

Vigenjevic [9] presented a new and improved compound beam element (CBE2) for transient hybrid finite element analysis. The element is a combination of an elastic beam and two non-linear rotary springs whose behaviour in the elastic/plastic and deep collapse range was controlled by inputted moment-rotation curves and a load interaction curve. Element stiffness matrix has been derived and its dependency on spring behavior was explained and tests were designed so that structural components collapse under biaxial bending and torsion. They not only concluded that CBE2 was more accurate than CBE1 but also that it does not suffer from the stability problems present in the formulation of CBE1.

Vogwell and Minguez [10] gave the comparison of different techniques for determining the shaft strength of fillet welded lap-joints under eccentric shear loading as the benefit of having torsionally closed, continuous fillet weld seam in preference to a torsionally open joint. The validity of generally using analysis based on simple torsion theory, as widely proposed in numerous design texts, was questioned and the alternative of using tubular, thin walled section and thin rectangular member torsion theory was investigated. The accuracies of the various compared with those given by a finite element analysis.

Nopolitano *et.al* [11] compared the performance of two concured damped composite torsion shafts which were light in weight, stiff and damped structural components. First shaft uses the extension twist coupling mechanism of off-angle composite materials to enhance the performance of a damping material and the second shaft uses a constraining layer embedded inside the shaft that floats between two layers of damping material and finite element analysis was used to determine the optimal damping material shear modulus and ply orientation to maximize shafts imaginary stiffness. Four shafts in total were built and modal tests were performed while both damping concepts provide significant levels of damping, the performance of each was hindered due to the increase in shear modulus of the damping material as it was occurred with the composite material.

Zhou and Clode [12] studied the temperature distribution in a hot torsion specimen. An aluminium alloy 5252 for different twist rates using finite element analysis was used. They also studied the initial temperature and specimen geometry and suggested the procedure for least heat generation. A comparison of the predicted ones with the obtained experimental results was done.

Maeda *et.al* [13] investigated the flexure torsion coupling stiffness on the vibrational characteristics using the Laser Holographic Interferometry on two special types of angle-ply specimens. The theoretical analysis by a finite element method was also conducted to support the experimental results. It was found that the effect of coupling stiffness on the natural frequencies were comparatively small. On the other hand, the mode shapes were strongly affected by the coupling terms depending on both the fiber orientation and the aspect ratio of a cantilevered laminate.

Kim and Kim [14] studied the topology optimization in the design of thin walled beam sections, useful in identifying the direction and location of stiffeners. In formulating the topology optimization problems, a simple power law was used for the relation between the density of an element with a hole and the mechanical properties of the element. The sensitivity of the torsional rigidity was obtained by the finite element model of the St. Venant torsion problem. Euler's beam theory was used for the sensitivity analysis of the bending rigidities.

Hashemi and Richard [15] studied the Dynamic Finite Element (DFE) formulation for the free vibration analysis of bending-torsion coupled beam. First, the exact solution of the differential equations governing the uncoupled vibrations of a uniform beam was found. These solutions as basis functions lead to the appropriate frequency dependent shape functions which could then be utilized to find the nodal approximations of variables. Principle of virtual work, the elementary dynamic stiffness matrix (DSM) were then obtained which has both mass and stiffness properties. The implementation of the derived DFE matrices in a program was discussed with a particular reference to the Wittrick-Williams algorithm. Study was demonstrated by illustrative

examples where substantial amount of coupling between bending and torsion was highlighted. Numerical checks were also published.

Wang *et.al* [16] tested the camshafts of the Rover Vehicles for the cyclic bending and torsion using finite element. Fatigue limit was predicted using a new technique, crack modeling. The method uses a linear elastic finite element analysis to derive an equivalent stress intensity factor (k) for stress concentrations in components. K was calculated without introducing a crack into the component: the stress field around the maximum stress point was examined and compared to that for a standard centre-cracked plate. Two designs under two loading modes were tested and further modifications were suggested.

Kuang and Ng [17] analyzed the dynamic performance of asymmetric shear-wall structures, replacing it by and equivalent thin-walled beam with lateral flexures and torsional deformations. Due to the asymmetry of the floor plan, the natural vibration of a structure was a coupled vibration, where lateral flexure vibrations in two orthogonal principal directions couple with a warping torsion vibration. Based on the continuum technique and the D'Alembert's principle, governing differential equations of natural vibration and the corresponding eigen value problem for asymmetric multi-bend wall structure were derived. Glerkin Approach was used to find the solution of coupled vibration of generally asymmetric shear-wall structure and for estimation of the coupled natural frequencies and associated mode shape in coupled vibration. Results were obtained theoretically and through finite element analysis and were compared. They were found in good agreement with each other.

Miyamura [18] presented the experimental and bifurcation analysis of wrinkling on circular stretched membrane under in-plane torsion. Test membranes are the orthotropic PVC coated textile and isotropic polyester film. Stresses were measured using non-linear finite element method and compared with the experimental results. These showed that the tension field was found in wrinkled membrane.

Lennon and Das [19] formulated the torsional displacement and buckling of a sector of a cylinder of half axial height, and of circumferential arc angle that would divide into 360°. Elastic-Plastic limit point finite element tests were carried out for studying the effect of stiffness on post buckling behavior in torsion. A stringer stiffened cylinder was subjected to many combinations of axial force and surface pressure in the elastic range of response and then tested to failure in torsion to investigate the effects of axial and surface pressure loads on the resistance to plastic collapse in torsion.

Katori [20] computed the shear centre of an arbitrary thin-walled cross-section using finite element method, considering the coupling problem of shearing and torsional deformation.

Li *et.al* [21] used the finite element analysis to design the cross-section of the shafts subjected to torsion. They developed two basic procedures to seek full stress and iso-strength design: either progressively removing the least efficient material from the design domain or gradually shifting material from the least efficient (under-utilized) location to the most efficient (over-utilized) location, keeping the cross-section area constant. Former leads to the remaining material being more effectively utilized and the later results in the material being more intelligently redistributed. Number of examples were given in this regards.

Savaidis *et.al* [22] presented a finite element analysis for a notched shaft subjected to non proportional synchronous multi-axial loading (tension/torsion). For simplicity one of the loading components was kept constant while the other was cyclic. The boundary value problem was solved by using the commercial finite element program system ABAQUS. A parametrical study was carried out and the numerical results were presented.

Wang *et.al* [23] presented an analytical method to solve the elastodynamic problem of a finite-length orthotropic hollow cylinder subjected to a torsional impact. The elastodynamic solution was composed of a quasi-static solution of homogeneous

equation satisfied with the non-homogeneous boundary condition. The quasi-static solution could be obtained by directly solving the quasi-static equation satisfied with the non-homogeneous boundary condition. The solution of a non-homogeneous dynamic equation was obtained by means of a finite Hankel transform to a radial variable z. Thus the elastodynamic solution of the finite length of an orthotropic hollow cylinder subjected to a torsion impact was obtained. A dynamic finite element for the same problem is carried out by applying the ANSYS finite element systems. A comparison of both the theoretical and finite element analysis results was made and the suitability of the theoretical method was checked.

Ellis *et.al* [24] gave the results of full scale torsion tests on rectangular hollow sections (RHS). Observed torque-twist behavior was compared with that of the predicted one and the significant differences were highlighted and examined. The behaviour predicted by the FE models were shown to be identical to that predicted one by Marshall's thick wall theory, which forms the basis of the British and European design procedures. However, even though the experimental measurements agreed with FE and the theoretical predictions were in the elastic range, the measurements of torsional capacity was significantly lower than those calculated, and this has important implications for design that may be wider than just torsion of RHS. A number of potential causes for this behaviour were examined.

Sapountzakis and Mokos [25] developed a Boundary Element Method (BEM) for non uniform torsion of composite bars of arbitrary variable cross-section, subjected to concentrated or distributed twisting moment and edges restrained by the most general linear tosional boundary conditions. Both variable warping and torsion constants together with the torsional shear stresses and the warping normal and shear stresses were computed numerical results were given to illustrate the method and demonstrate its efficiency and accuracy.

Shokrieh *et.al* [26] studied the torsional stability of a composite drive shaft used in various products such as cars, helicopters, cooling towers etc. Here the calculation of

the buckling torque of composite shaft drive and finite element analysis was performed and the numerical results thus obtained were analytically and experimentally compared. Finally, the reduction of torsional natural frequency of a composite drive shaft due to an increase in the torque was studied.

Kim *et.al* [27] gave the element stiffness matrix for flexure-torsion free vibration analysis of a thin walled beam with non-symmetric cross-sections on two types of elastic foundation. Deformation effect in beam is due to the shear force and the restrained warping torsion and due to the coupled effects between them, rotary inertia effect and the flexure torsion coupling effects due to the non-symmetric cross-sections. Equations of motion and force deformation were derived from the energy principle and explicit expressions for displacement parameters were derived based on power series expansions of displacement components and the exact dynamic elements stiffness matrix was determined using force-deformation relationships. Numerical solutions were presented and compared with analytical solutions. The influences of the coupled shear deformation on the vibrational behaviour of non-symmetric beam on elastic foundation were also investigated.

Sapountzakis [28] worked on the torsional vibrations of composite bars of variable cross-section and developed a Boundary Element Method (BEM) for the non-uniform torsional vibration problem of doubly symmetric composite bars of arbitrary variable cross-section. The composite bar consisted of materials in contact, each of which could surround a finite number of inclusions. The materials had different elasticity and shear moduli and were firmly bonded together. They considered both free and forced torsional vibration and presented numerical examples to illustrate the method and demonstrate its efficiency and accuracy.

Sapountzakis [29] worked on the torsional vibrations of composite bars of constant cross-section and developed a Boundary Element Method (BEM) for the non-uniform torsional vibration problem of doubly symmetric composite bars of arbitrary variable cross-section. The materials had different elasticity and shear moduli and were

firmly bonded together. The beam was subjected to an arbitrarily distributed dynamic twisting moment, while its edges were restrained by the most general linear torsional boundary conditions. Considering both free and forced torsional vibration. Numerical examples were presented to illustrate the method and demonstrate its efficiency and accuracy.

Cheong *et.al* [30] experimentally and numerically evaluated the mechanical properties of the golf shafts. The degree of torsion was measured by applying the twisting moment, 13.72 (kgf cm), to the tip. The frequency of vibration was measured by adding a mass to the tip of a shaft and shaking it. The position of the kick point, that is, the maximum deflection point was measured by compressing the tip. The composite structure of a golf shaft made of fiber-reinforced plastics was modeled and the mechanical performance of the structure was numerically evaluated. Both a linear static and dynamic analysis for a golf shaft was performed. Comparing the presented numerical results with experimental data, the effects of major parameters on the performance of golf shafts were also discussed.

Gu and Chan [31] formulated a tangent stiffness matrix for the geometrically non-linear analysis of the space beam column elements allowing for the axial-flexural, lateral-torsional and axial-torsional buckling. Three deformation matrices were derived for moderately large rotations in practical three-dimensional space frames subjected to axial force and moments. These matrices were functions of the element deformations and include the coupling among axial, lateral and torsional deformations. Proposed matrices were used together with linear and geometric stiffness matrices for beam elements to study large deflection behavior of space frames which comprises of members of negligible warping effect. Numerical examples were also given.

Troyani N. et.al [32] studied the finite element mesh orientation in terms of the effects it may have on solution accuracy in torsion problems. This work studied the effect of triangular finite element mesh orientation with regards to the torsion of non-circular machine elements and structural elements in terms of maximum shearing stress

computation accuracy. Two sets of results for two specific orientations are reported: mesh orientation approximately perpendicular to the membrane contour lines and mesh orientation in a direction approximately parallel to the membrane contour lines. This study demonstrates that mesh orientation may have important consequences on the accuracy of the solution for the type of stress estimates treated in this work.

2.2 SUMMARY OF LITERATURE REVIEW

From the extensive literature review discussed above, it is seen that finite element method (FEM) is used as a tool for the analysis of various components when subjected to different loading conditions. Mesh generation play a very important role in the accuracy of the results obtained from finite element method.

The present work is step towards the improvement of accuracy to be done by analyzing the orientation of the mesh in a simple component. This work can further be extended to more complicated problems.

ANALYSIS CHAPTER 3

3.1 INTRODUCTION

Finite element (FE) methods represent a powerful tool for both engineering analyses and mathematical analyses; however, they also possess certain limitations. Frequently, special solution devices can overcome these limitations. In the present work, the accuracy exhibited by a particular form of FE mesh manipulation is examined when applied to the computation of maximum shearing stresses in torsional problems.

Low order triangular and quadrilateral elements are often preferred in structural mechanics. To this end, a particular aspect of triangular finite element meshes is studied; namely, mesh orientation (diagonal orientation) in non-circular cross sections in order to establish the effect of this aspect on solution quality. This type of mesh sensitivity analysis is of interest in both mechanical and structural engineering.

In the procedure that follows, the mesh orientation process is guided by the analogy that exists between the torsion of prismatic member's problem and the deflection of a membrane problem, the latter being a Poisson type of problem, studying both the effect of aligning the FE mesh in directions approximately perpendicular to the edge of the member (square cross-section) and also the effect of aligning the FE mesh approximately parallel to the edge of the member (square cross-section).

3.2 FEM ANANLYSIS FOR TORSION SHAFTS

Consider a prismatic rod of arbitrary cross-sectional shape which is subjected to a twisting moment M as shown in Fig.3.1. The problem is to determine shearing stresses τ_{xz}, τ_{yz} Fig 3.2 and the angle of twist per unit length, α. It can be shown that the solution of such problems, with simple connected cross-sections, reduces to solving the two dimensional equation.

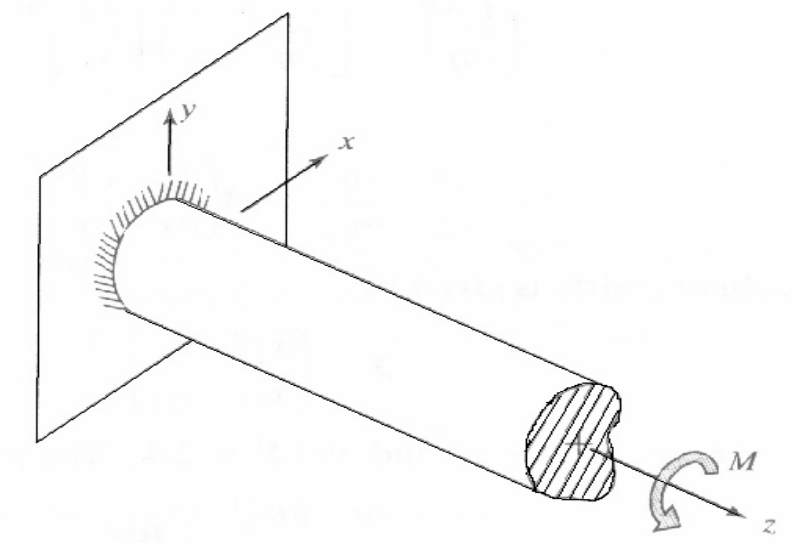

Fig. 3.1 A rod of arbitrary cross section subjected to a torque

$$\frac{\partial^2\theta}{\partial x^2}+\frac{\partial^2\theta}{\partial y^2}+2=0 \text{ in } A \quad \text{..... (3.1)}$$

$$\theta = 0 \text{ on } S \quad \text{..... (3.2)}$$

where, A is interior and S is the boundary of the cross-section. In eq.3.2, θ is called the stress function, since once θ is known, then shearing stresses are obtained as

$$\tau_{xz} = G\alpha\frac{\partial\theta}{\partial y} \qquad \tau_{yz} = -G\alpha\frac{\partial\theta}{\partial x} \quad \text{..... (3.3)}$$

with α determined from

$$M = 2G\alpha\iint_A \theta dA \quad \text{..... (3.4)}$$

where G is the shear modulus of the material. The finite element method for solving eq.3.1 and eq.3.2 will now be given.

The stress function θ within a triangular element is interpolated as

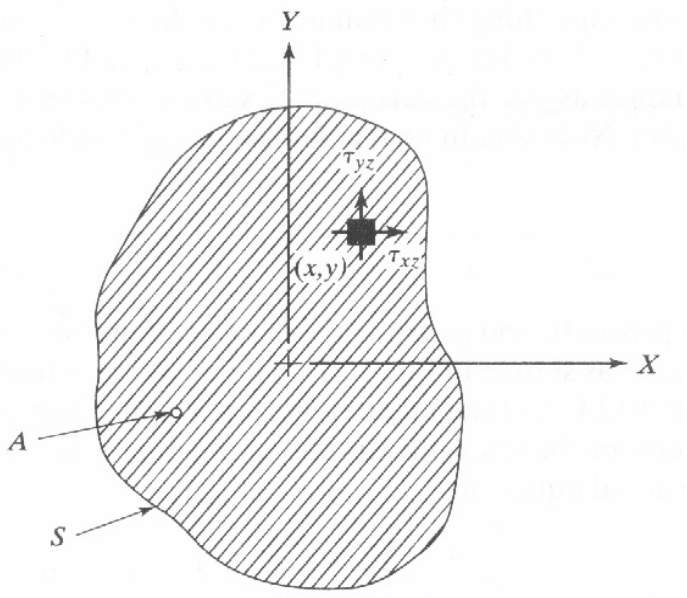

Fig. 3.2 Shearing stress in torsion

$$\theta = N\theta^e \quad \text{..... (3.5)}$$

where $N = [\xi, \eta, 1-\xi-\eta]$ are the usual shape functions, and $\theta^e = [\theta_1, \theta_2, \theta_3]^T$ are the nodal values of θ. Furthermore, we have the isoparametric relations

$$x = N_1 x_1 + N_2 x_2 + N_3 x_3 \quad \text{..... (3.6)}$$

$$y = N_1 y_1 + N_2 y_2 + N_3 y_3 \quad \text{..... (3.7)}$$

$$\begin{Bmatrix} \frac{\partial\theta}{\partial\xi} \\ \frac{\partial\theta}{\partial\eta} \end{Bmatrix} = \begin{bmatrix} \frac{\partial x}{\partial\xi} & \frac{\partial y}{\partial\xi} \\ \frac{\partial x}{\partial\eta} & \frac{\partial y}{\partial\eta} \end{bmatrix} \begin{Bmatrix} \frac{\partial\theta}{\partial x} \\ \frac{\partial\theta}{\partial y} \end{Bmatrix} \quad \text{..... (3.8)}$$

or

$$\begin{bmatrix} \frac{\partial\theta}{\partial\xi} & \frac{\partial\theta}{\partial\eta} \end{bmatrix}^T = J \begin{bmatrix} \frac{\partial\theta}{\partial x} & \frac{\partial\theta}{\partial y} \end{bmatrix}^T \quad \text{..... (3.9)}$$

where the Jacobean matrix **J** is given by

$$J = \begin{bmatrix} x_{13} & y_{13} \\ x_{23} & y_{23} \end{bmatrix} \quad \text{..... (3.10)}$$

with $x_{ij} = x_i - x_j, y_{ij} = y_i - y_j$ and $|\det J| = 2A_e$. The preceding equations yield

$$\begin{bmatrix} \frac{\partial \theta}{\partial x} & \frac{\partial \theta}{\partial y} \end{bmatrix}^T = B\theta^e \quad \text{..... (3.11)}$$

or

$$\begin{bmatrix} -\tau_{yz} & \tau_{xz} \end{bmatrix}^T = G\alpha B\theta^e \quad \text{..... (3.12)}$$

where

$$B = \frac{1}{\det J}\begin{bmatrix} y_{23} & y_{31} & y_{12} \\ x_{32} & x_{13} & x_{21} \end{bmatrix} \quad \text{..... (3.13)}$$

3.2.1 COMPLEMENTARY POTENTIAL ENERGY APPROACH

The solution of eq.3.1 is equivalent to minimizing the complementary potential energy Π in the rod. For the length of the rod,

$$\Pi = G\alpha^2 \iint_A \left\{ \frac{1}{2}\left[\left(\frac{\partial \theta}{\partial x}\right)^2 + \left(\frac{\partial \theta}{\partial y}\right)^2 \right] - 2\theta \right\} dA \quad \text{..... (3.14)}$$

the element stiffness matrix an load vectors can now be derived from Π. The constant $G\alpha^2$ multiplying Π may be disregarded.

Using eq.3.11, we have

$$\left(\frac{\partial \theta}{\partial x}\right)^2 + \left(\frac{\partial \theta}{\partial y}\right)^2 = \begin{bmatrix} \frac{\partial \theta}{\partial x} & \frac{\partial \theta}{\partial y} \end{bmatrix} \begin{Bmatrix} \frac{\partial \theta}{\partial x} \\ \frac{\partial \theta}{\partial y} \end{Bmatrix} \quad \text{..... (3.15)}$$

$$= \theta^{e^T} B^T B \theta^e \quad \text{..... (3.16)}$$

Thus, the strain energy term in Π becomes

$$\iint_A \left\{ \frac{1}{2} \left[\left(\frac{\partial \theta}{\partial x} \right)^2 + \left(\frac{\partial \theta}{\partial y} \right)^2 \right] \right\} dA = \sum_e \frac{1}{2} \theta^{e^T} k \theta^e \quad \text{..... (3.17)}$$

where $k = A_e B^T B$

the load term becomes

$$\iint_A 2\theta dA = \sum_e \left(2 \int_e N dA \right) \theta^e \quad \text{..... (3.18)}$$

Since $\int_e N_i dA = A_e / 3$, we have,

$$\iint_A 2\theta dA = \sum_e \theta^{e^T} \text{ f} \quad \text{..... (3.19)}$$

where

$$\text{f} = \frac{2A_e}{3} \begin{bmatrix} 1 & 1 & 1 \end{bmatrix}^T \quad \text{..... (3.20)}$$

The expression for Π is now given by

$$\Pi = \frac{1}{2} \theta^T K \theta - \theta^T F \quad \text{..... (3.21)}$$

where $K = \sum_e k, F = \sum_e$ f are assembled in the usual manner using element connectivity. The minimization of Π is subject to the boundary conditions $\Psi_i = 0$ for every node *i* on the boundary. The resulting equation is

$$K\theta = F \quad \text{..... (3.22)}$$

where K, F are then modified to account for boundary conditions, either by the penalty or elimination approaches. Once θ is known, we can determine the shearing stresses from eq.3.12.

3.3 ALGORITHM OF THE PROGRAM

The following steps are followed for finding the solution of torsional problem using finite element analysis.

1. Input the dimensions of the square cross-sectional torsional problem.
2. Input the number of triangular elements with their initial connectivity.
3. Allocate memory for the following required matrices.

- x [total no. of joints] and y [total no. of joints] for the coordinates.
- Connectivity matrix given by connect [total no. of members] [no. of nodes/element], which gives the connectivity between different members.
- Element stiffness matrix given by estiff [total no. of nodes/element x dof] [total no, of nodes/element x dof].
- System matrix given by a [total no. of joint x dof] [total no. of joint x dof].
- Boundary condition matrix, given by bcc [total no. of joints x dof].
- Load matrix given by b [total no. of joints x dof].

4. First of all the mesh is generated. this is done in two steps:

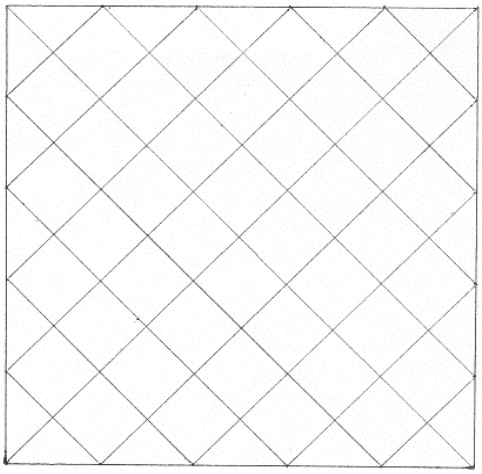

(a)

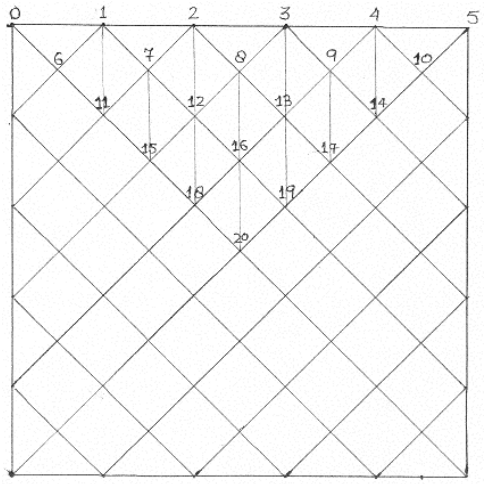

(b)

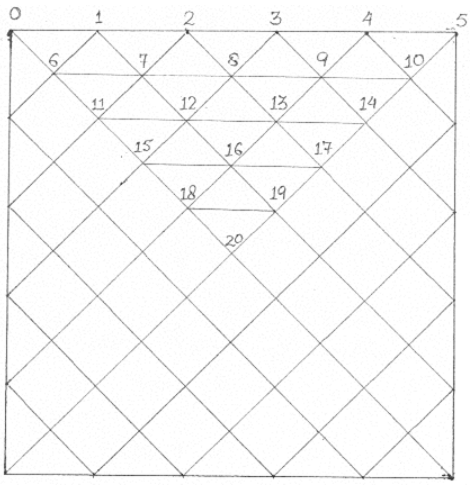

(c)

Fig.3.3 Mesh Generation (a) Basic structure, (b) Perpendicular Mesh and, (c) Parallel Mesh

Step1: To generate element connectivity data.

Step 2: Nodal coordinate data.

This will automatically give connectivity between different elements and the x, y coordinate values according to number of divisions in x, y direction.

A brief description is given below:

- First of all give numbers to all the nodes starting with 0.
- Coordinates are calculated by dividing the rectangular cross-section [1/4 part of the cross-section into best suited number of triangular elements.

5. Starting from the first element, find the element stiffness matrix for each element, using eq.

$$K_1 = \begin{bmatrix} x_{11} & x_{12} & x_{13} \\ x_{21} & x_{22} & x_{23} \end{bmatrix}, \theta_1 = \begin{bmatrix} \theta_1 \\ \theta_2 \\ \theta_3 \end{bmatrix}, F_1 = \begin{bmatrix} a_1 \\ a_2 \\ a_3 \end{bmatrix}$$

6. Assemble the entire element stiffness matrix into a system stiffness matrix using the assembly procedure.

$$K=\begin{bmatrix} y_{11} & y_{12} & \cdots & \cdots & y_{121} \\ y_{21} & y_{22} & \cdots & \cdots & y_{221} \\ \vdots & \vdots & \vdots & \vdots & \vdots \\ \vdots & \vdots & \vdots & \vdots & \vdots \\ y_{211} & y_{212} & \cdots & \cdots & y_{2121} \end{bmatrix}, \theta=\begin{bmatrix} \theta_1 \\ \theta_2 \\ \vdots \\ \vdots \\ \theta_{21} \end{bmatrix}, F=\begin{bmatrix} b_1 \\ b_2 \\ \vdots \\ \vdots \\ b_{21} \end{bmatrix}$$

7. Now modify the system stiffness matrix according to the boundary conditions. For example, if i[th] node is fixed then all the values of rows and columns of system stiffness at i*2 are substituted zero and at a [i*2] [i*2], value 1 is substituted. Same way in load matrix at i*2 value of row, load is substituted zero.
8. Now matrix is solved using the solver (Gauss Elimination Method is used in this case).
9. This will give the values of nodal deflection, θ for all the nodes of the square cross-section.
10. Now the value of twist is calculated by

$$M = 2G\alpha\left[\sum_e \frac{A_e}{3}\left(\theta_1^e + \theta_2^e + \theta_3^e\right)\right].$$

11. Then the value of shear stress is calculated in yz and xz plane using

$$\begin{bmatrix} -\tau_{yz} & \tau_{xz} \end{bmatrix}^T = G\alpha B\theta^e$$

where

$$B = \frac{1}{\det J}\begin{bmatrix} y_{23} & y_{31} & y_{12} \\ x_{32} & x_{13} & x_{21} \end{bmatrix}.$$

12. Mesh generation in the case of circular cross section shaft is done as:

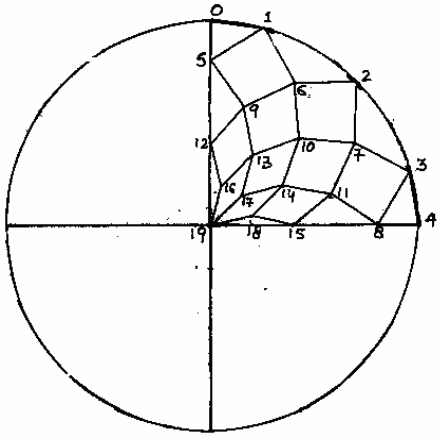

(a)

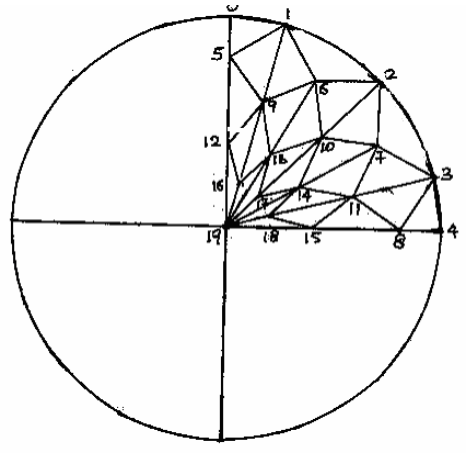

(b)

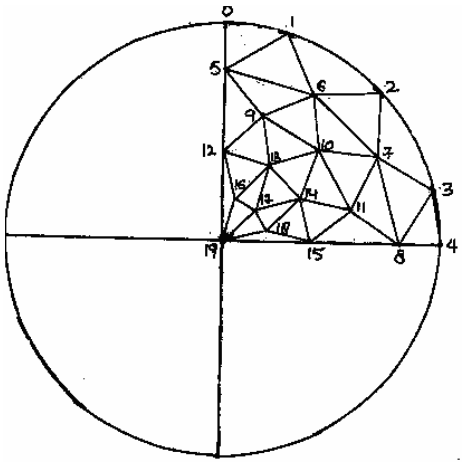

(c)

Fig.3.4 Mesh Generation (a) Basic structure, (b) Perpendicular Mesh and, (c) Parallel Mesh

After the mesh is generated a similar procedure as stated above for the calculation of the values of θ and their respective stresses is used and the results have been graphically plotted.

4.1 INTRODUCTION

In the following section the results of the program are taken applying conditions as per the work of N.Troyani *et. al* [32]. These results are then validated based on methodology given in the previous chapter. The results presented are for twist and shear stress for two types of mesh orientation for triangular elements based on torsional problem.

4.2 RESULT VALIDATION AND DISCUSSION

The technique of finite element has been applied to the analysis of the results of mesh orientation when a square cross-section member is subjected to torsion. In this two types of triangular meshes are taken, viz.

- Parallel to the edge.
- Perpendicular to the edge.

A square cross-section shaft is firstly divided into four major triangles by two diagonals. One of the triangles is further divided into triangular elements based on a specific orientation. Node numbers are given to all the edges. Coordinates at various nodes are calculated based on their respective connectivity. Thereafter, the boundary conditions are applied as shown in the Fig. 4.1.

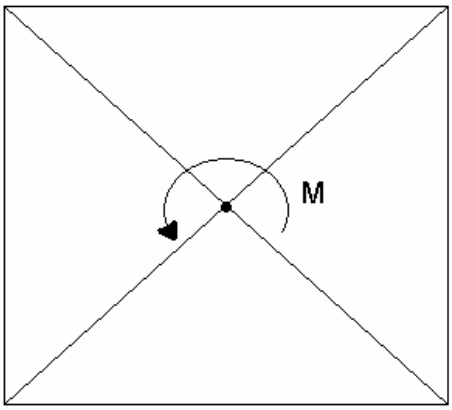

Fig. 4.1 A finite element model of a quadrant of square cross-section

After applying the FEA procedure the values of θ on the respective nodes were calculated. The various values of θ for the two types of orientation have been tabulated below:

Table 1.Comparison of θ for perpendicular and parallel orientation

Node No.	θ(in degrees) for parallel orientation	θ (in degrees) for perpendicular orientation
0.	2.6908	2.6373
1.	3.0965	3.0847
2.	4.2604	4.2646
3.	4.8046	4.7979
4.	5.3943	5.3368
5.	5.5933	5.4821
6.	2.5575	2.5039
7.	3.9079	3.8463
8.	4.4796	4.4162
9.	4.99638	4.9131
10.	5.46	5.3487
11.	3.637	3.5797
12.	4.0749	4.0179
13.	4.4981	4.4327
14.	5.05807	4.9725
15.	3.7747	3.7223
16.	3.7372	3.6866
17.	4.3794	4.31502
18.	2.9123	2.8739
19.	3.06348	5.022
20.	0	0

Afterwards, considering these values of θ, twist (α) has been calculated using the formula

$$M = 2G\alpha\left[\sum_e \frac{A_e}{3}\left(\theta_1^e + \theta_2^e + \theta_3^e\right)\right]$$

$$\alpha_P = 0.005307$$

$$\alpha_{PD} = 0.005459$$

Using this value of twist in the formula, $\left[-\tau_{yz} \quad \tau_{xz}\right]^T = G\alpha B\theta^e$ various values of shear stress has been calculated.

Values of τ_{yz} and τ_{xz} has been shown in table 2 and 3:

Table 2.Comparison of τ_{yz} for perpendicular and parallel orientation

Node No.	τ_{yz} for parallel orientation	τ_{yz} for perpendicular orientation
0.	8.612	9.77
1.	28.6677	36.1731
2.	28.6677	22.4509
3.	12.137	12.8797
4.	12.1374	12.0081
5.	10.9693	8.6983
6.	10.9693	13.0034
7.	9.8436	10.55
8.	9.8436	8.4752
9.	4.2247	3.1708
10.	9.2952	8.9351
11.	9.2952	10.1995
12.	8.9859	1.4648
13.	8.9859	16.6533
14.	11.886	7.9187
15.	11.886	15.6537
16.	0.7976	-12.0737

17.	0.7976	10.5145
18.	13.6347	1.7794
19.	13.6347	25.6623
20.	3.2092	-45.0089
21.	3.2092	51.4797

Table 3.Comparison of τ_{xz} for perpendicular and parallel orientation

Node No.	τ_{xz} for parallel orientation	τ_{xz} for perpendicular orientation
0.	-14.273	-15.593
1.	5.7818	10.8087
2.	17.1664	10.8087
3.	-2.8305	-5.3872
4.	-5.0482	-5.3872
5.	-2.8305	-7.9755
6.	-10.1831	-7.9755
7.	-7.0553	-7.956
8.	-7.2241	-7.9565
9.	-1.4363	-2.6521
10.	-2.20602	-2.70703
11.	-3.44702	-2.70703
12.	-8.1996	-15.9305
13.	-23.3234	-15.9305
14.	-9.26644	-13.0602
15.	-16.926	-13.0602
16.	-13.5398	-24.9802
17.	-35.822	-24.9802
18.	-18.6747	-30.8039
19.	-47.2406	-30.8039

20.	-31.8151	-80.5037
21.	-126.86	-80.5037

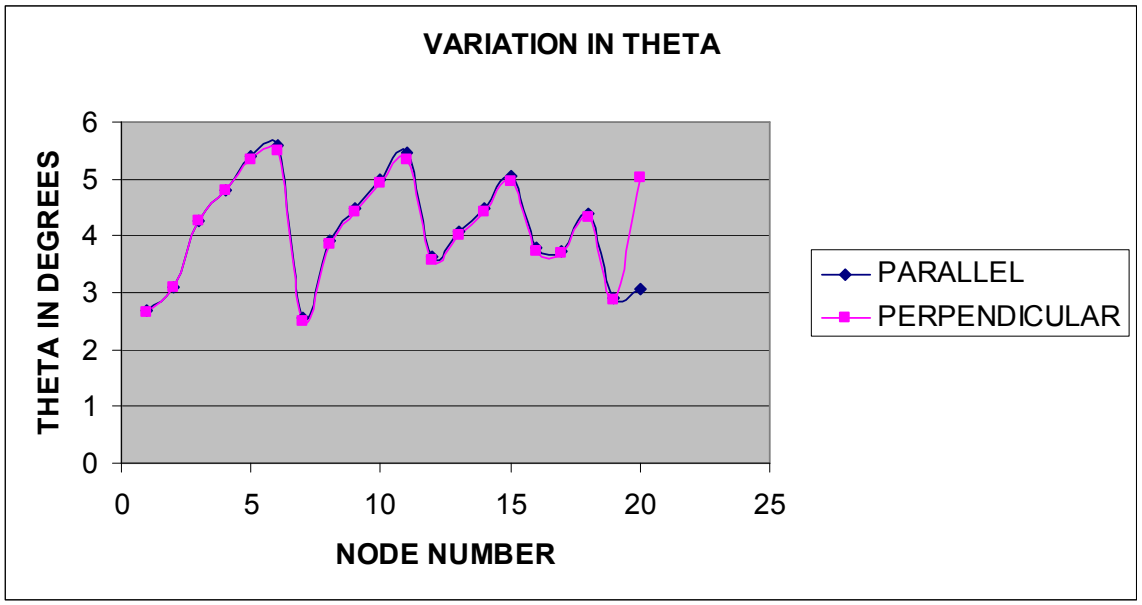

Fig. 4.2 Comparison of θ for perpendicular and parallel orientation

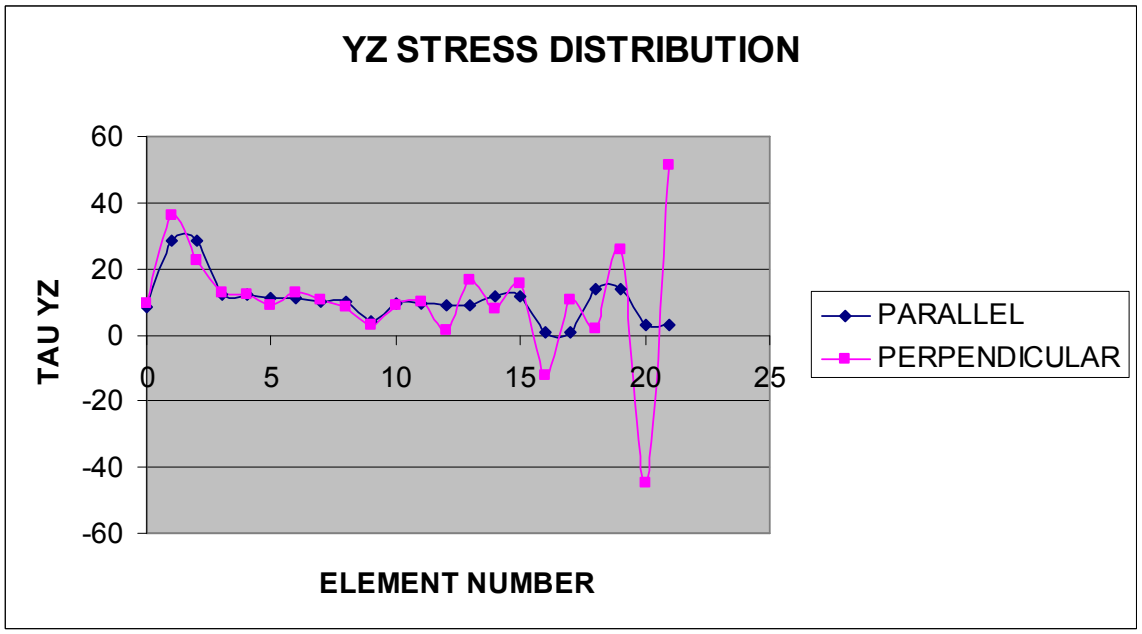

Fig. 4.3 Comparison of τ_{yz} for perpendicular and parallel orientation

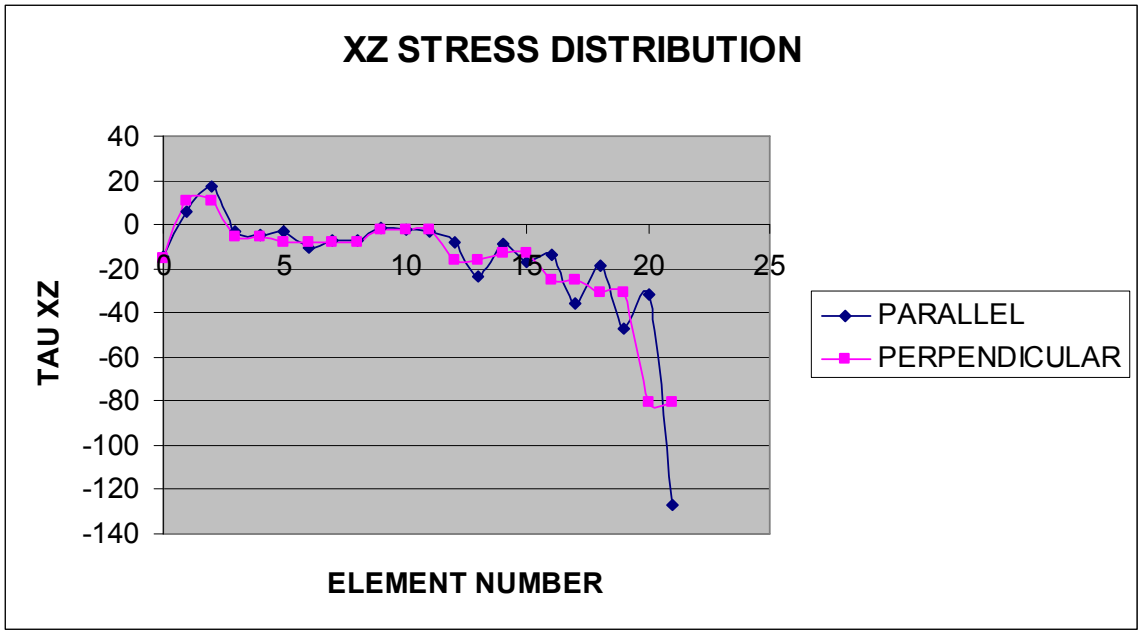

Fig.4.4 Comparison of τ_{xz} for perpendicular and parallel orientation

Observing these graphs we can conclude that the values obtained by considering the triangular mesh which is parallel to the edge of the square cross-section shows more accurate and smooth results as compared to that of the results obtained when the triangular mesh is perpendicular to the edge of the square cross-section.

Now, taking a circular cross-section shaft and discretizing it into four quarters. One of the quarter is further divided into triangular elements based on a specific orientation. Node numbers are given to all the edges. Coordinates at various nodes are taken based on their respective connectivity. Thereafter, the boundary conditions are applied as shown in the Fig. 4.5.

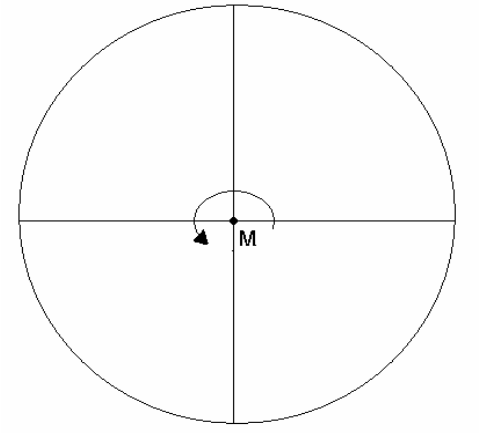

Fig. 4.5 A finite element model of a quadrant of circular cross-section

After applying the FEA procedure the values of θ on the respective nodes were calculated. The various values of θ for the two types of orientation have been tabulated below. Similar procedure as applied above is used to do the calculations. Various tables along with their graphs are shown below:

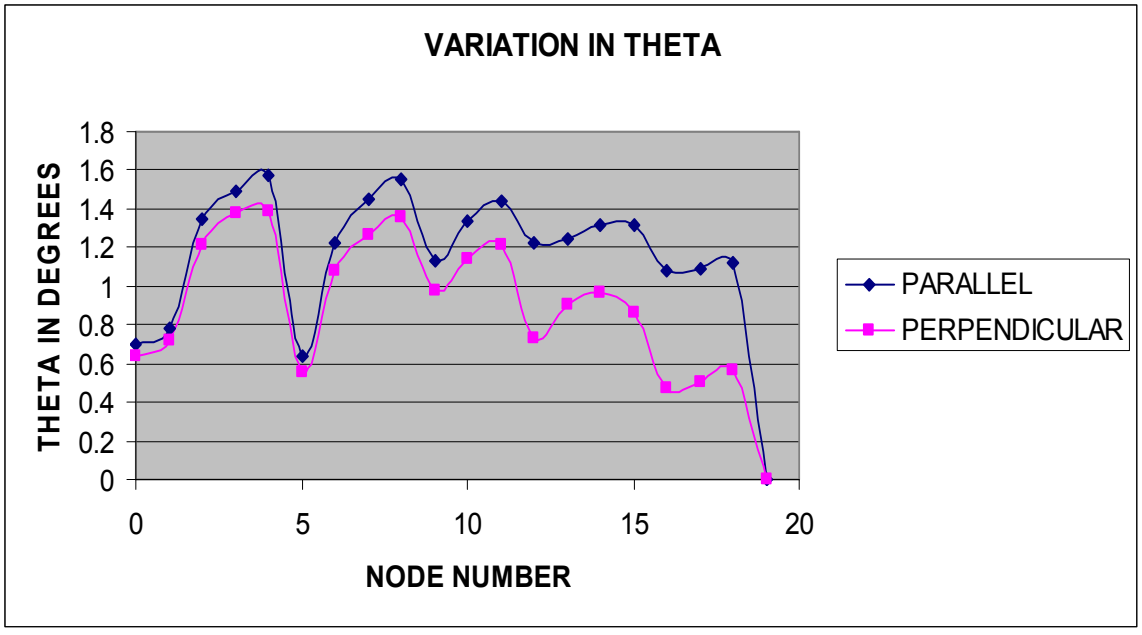

Fig. 4.6 Comparison of θ for perpendicular and parallel orientation

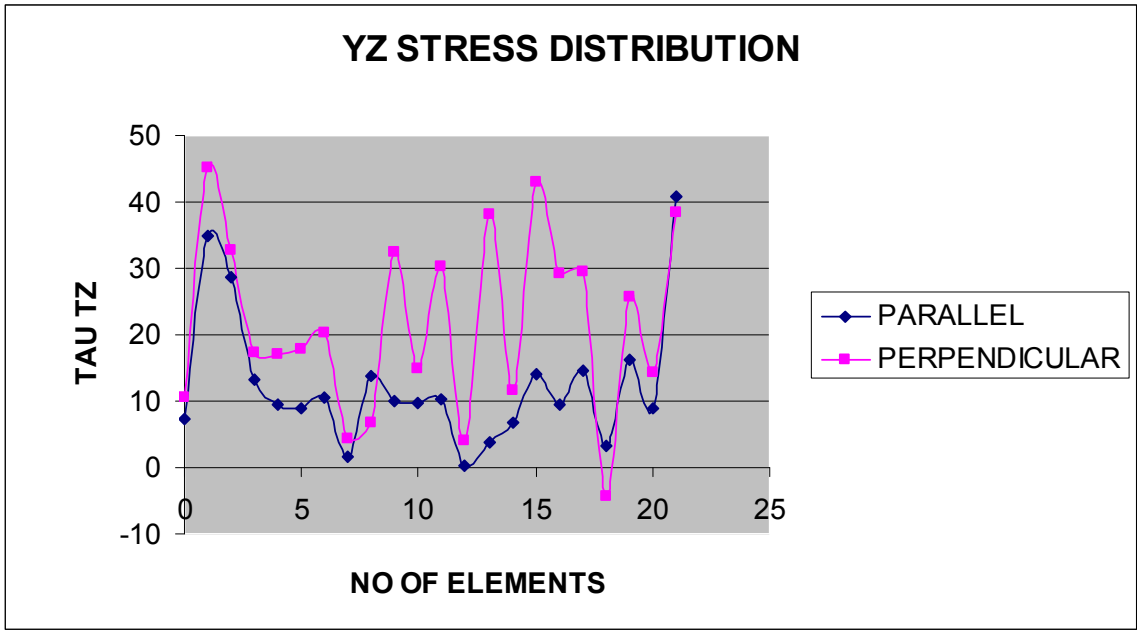

Fig. 4.7 Comparison of τ_{yz} for perpendicular and parallel orientation

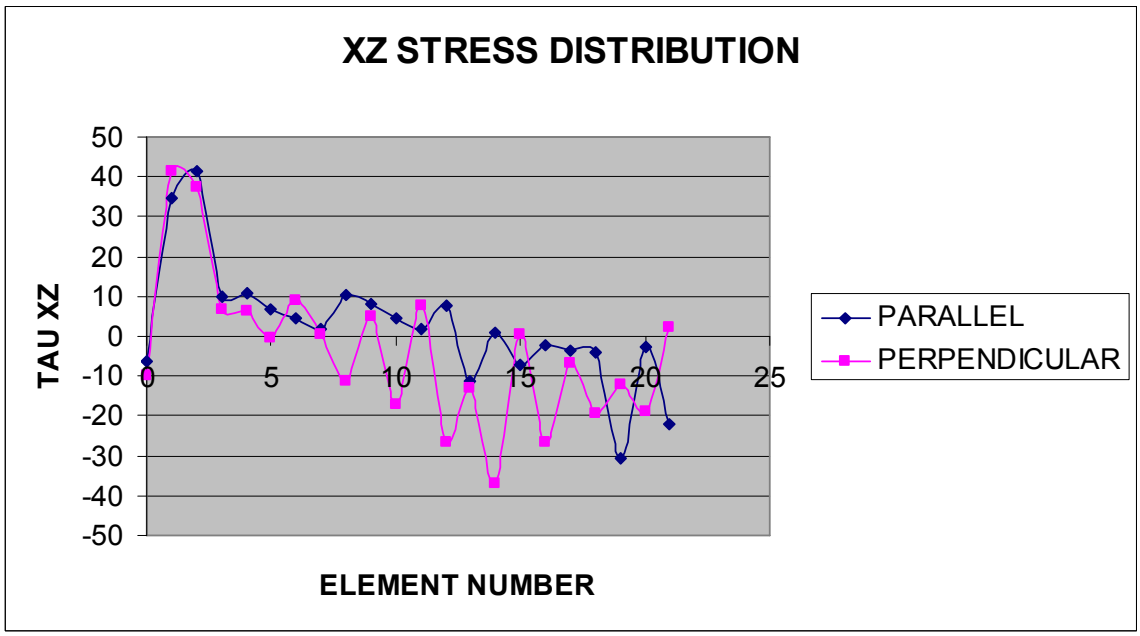

Fig. 4.8 Comparison of τ_{xz} for perpendicular and parallel orientation

Observing these graphs we can conclude that in the case of circular cross-section shafts the values obtained by considering the triangular mesh which is parallel to the

circumference of the shaft shows more accurate and smooth results as compared to that of the results obtained when the triangular mesh is perpendicular to the circumference of the shaft.

CONCLUSION CHAPTER-5

This chapter gives the conclusions as obtained from the results of the analysis of mesh orientation of square cross-sectional shaft subjected to torsion using finite element technique.

5.1 CONCLUSION

- The results obtained from the finite element model demonstrates that triangular mesh which is parallel to the edge of the square cross-section shows more accurate and smooth results as compared to that of the results obtained when the triangular mesh is perpendicular to the edge of the square cross-section.
- The result obtained from the finite element model of square and circular cross-sectioned shafts, demonstrates that the, technique can be subjected to the shafts of other cross-sections under different loading conditions.

5.2 FUTURE SCOPE

- This work can further be extended to other cross-sections subjected to torsion.
- This work can further be extended to 3D.
- Accuracy can be checked for other loading conditions.

BIBLIOGRAPHY

[1] S. Chandrakant Desai and F. John Abel, Introduction to Finite Element Method, East-West Edition, 1977.

[2] O.C. Zienkiewicz, The Finite Element Method, Tata McGraw-Hill Edition, London, 1979.

[3] J.N. Reddy, Finite Element Method, McGraw-Hill International Editions, 1993.

[4] S.Rajesekaran, Finite Element Analysis in Engineering Design,Wheeler Publishing,1994.

[5] U.C. Jindal, Introduction to Strength of Material, Galgotia Publications Pvt. Ltd., 1998.

[6] Sadhu Singh, Strength of Materials, Khanna Publishers, 1999.

[7] M. James Gere and P. Stephen Timoshenko ,Mechanics of Materials, CBS Publishers and Distributors, 2002.

[8] I.M. Smith and D.V.Griffiths, Programming the Finite Element Method, John Wiley and Sons Ltd., 2004.

[9] R. Tirupathi Chandrupatla and D. Ashok Belegundu, Introduction to Finite Elements in Engineering, Pearson Education , Singapore, 2004.

REFERENCES

[1] Nouailhas Dominique and Cailletaud Georges, "*Tension-Torsion Behavior of Single-Crystal Superalloys: Experiment and Finite Element Analysis"*, International Journal of Plasticity, Vol. 11, No. 4, pp. 451-470, 1995.

[2] Mentrasti L., "*Curved Thin-Walled Open-Closed Cross Section Beam with Finite Width",* International Journal of Engineering Sciences, Vol. 33, No. 4, pp. 497-524, 1995.

[3] Loughlan J. and Ata M., "*The Restrained Torsional Response of Open Section Carbon Fiber Composite Beams*", Composite Structures, Vol. 32, pp. 13-31, 1995.

[4] Hu Y., Jin X. and Chen B., "*A Finite Element Model for Static and Dynamic Analysis of Thin-Walled Beams with Asymmetric Cross-Section*", Computers and Structures, Vol. 61, No. 5, pp. 897-908, 1996.

[5] Morrell P.J.B., Riddington J.R., Ali F.A. and Hamid H.A., "*Influence of Joint Detail on the Flexural/Torsional Interaction of Thin-Walled Structures*", Thin Walled Structure, Vol. 24, pp 97-111, 1996.

[6] Nori Chandrasekhar V., McCarty Tyrus A. and Mantena P. Raju , "*Viberation Analysis and Finite Element Molding for Determining Shear Modulus of Pultruded Hybrid Composites*", Composites: Part B, 27B , pp 329-337, 1996.

[7] Mitsuya Y., Ohshima Y., & Nonogaki T., "*Coupling and Nonlinear Effects of Cantilever Deflection and Torsion Encountered when Simultaneously Measuring Vertical and Lateral Forces using the Scanning Probe Method*", Wear, Vol.211, pp 198-202, 1997.

[8] Loughlan J., and Ata M., "*The Constrained Torsional Characteristics of Some Carbon Fiber Composites Box- Beams*", Thin Walled Structures, Vol. 28, Nos. ¾, pp. 233-252, 1997.

[9] Vignjevic R., "*A Hybrid Approach to the Transient Collapse Analysis of Thin Walled Frameworks II*", Computational. Methods Applied Mechanical Engineering, Vol 148, pp.423- 437, 1997.

[10] Vogwell J., and Minguez J.M., "*Predicting Failure in Non-Continuous Weld Seams when used in Joints under Torsion Loading*", Engineering Failure Analysis, Vol. 4, No. 4, pp. 227-236, 1997.

[11] Napolitano K. L., Grippo W., Kosmatka J.B. and Johnson C.D., "*A Comparison of Two Cocured Damped Composite Torsion Shafts*", Composite Structures, Vol. 43, pp. 115-125, 1998.

[12] Zhou M. and Clode M.P., "*A Finite Element Analysis for the Least Temperature Rise in a Hot Torsion Test Specimen*", Finite Elements in Analysis And Design, Vol. 31, pp 1-14, 1998.

[13] Maeda Takenori, Baburaj Vijayan and Koga Tatsuzo, "*Dynamic Studies of Angle-Ply Laminates including Flexure-Torsion Coupling using Laser Holography*", Optics and Lasers in Engineering, Vol. 30, pp 191-198, 1998.

[14] Kim Yoon Young and Kim Tae Soo, "*Topology Optimization of Beam Cross Sections*", International Journal of Solids and Structures, Vol. 37, pp 477-493, 2000.

[15] Hashemi S. Mohammad and Richard Marc J., "*A Dynamic Finite Element (DFE) Method for Free Vibrations of Bending-Torsion Coupled Beams*",Aerospace Science Technology, Vol. 4, pp. 41-55, 2000.

[16] Wang G., Taylor D., Bouquin B., Devlukia J. and Ciepalowicz A., "*Prediction of Fatigue Failure in a Camshaft using the Crack Modeling Method*", Engineering Failure Analysis, Vol. 7, pp. 189-197, 2000.

[17] Kuang J.S. and Ng S.C., "*Coupled Lateral-Torsion Vibration of Asymmetric Shear-Wall Structures*", Thin-Walled Structures, Vol. 38, pp. 93-104, 2000.

[18] MIyamura Tomoshi, "*Wrinkling On Stretched Circular Membrane under In-Plane Torsion: Bifurcation Analyses and Experiments*", Engineering Structures, Vol. 23, pp. 1407-1425, 2000.

[19] Lennon R.F. and Das P.K., "*Torsional Buckling Behaviour of Stiffened Cylinders under Combined Loading*", Thin-Walled Structures, Vol. 38, pp. 229-245, 2000.

[20] Katori Hiroaki, "*Consideration of the Problem of Shearing and Torsion of Thin-Walled Beams with Arbitrary Cross-Section*", Thin-Walled Structures, Vol. 39, pp. 671-684, 2001.

[21] Li Qing, Steven Grant P., Querin Osvaldo M. and Xie Y.M., "*Stress Based Optimization of Torsional Shafts using an Evolutionary Procedure*", International Journal of Solids and Structures, Vol.38, pp. 5661-5677, 2001.

[22] Savaidis A., Savaidis G. and Zhang Ch., "*FE Fatigue Analysis of Notched Elastic-Plastic Shaft under Multiaxial Loading Consisting of Constant and Cyclic Components*", International Journal of Fatigue, Vol. 23, pp. 303-315, 001.

[23] Wang X., Xia X.h. and Hao W.H., "*An Elastodynamic Solution of Finite Long Orthotropic Hollow Cylinder under Torsion Impact*", Journal of Sound and Vibration, Vol. 267, pp. 67-86, 2003.

[24] Ridley-Ellis D.J., Owen J.S. and Davies G., "*Torsional Behaviour of Rectangular Hollow Sections*", Journal of Constructional Steel Research, Vol. 59, pp.641-663, 2003.

[25] Sapountzakis E.J. and Mokos V.G., "*Nonuniform Torsion of Composite Bars of Variable Thickness by BEM*", International Journal of Solids and Structures, Vol. 41, pp. 1753-1771, 2004.

[26] Shokrieh Mahmood M., Hasani Akbar and Lessard Larry B., "*Shear Buckling of a Composite Drive Shaft under Torsion*", Composite Structures, Vol. 64, pp.63-69, 2004.

[27] Kim Nam-II, Lee Ji-Hun and Kim Moon-Young, "*Exact Dynamic Stiffness Matrix of Non-Symmetric Thin-Walled Beams on Elastic Foundation using Power Series Method*", Advances in Engineering Software, Vol. 36, pp. 518-532, 2005.

[28] Sapountzakis Evangelos J., "*Torsional Vibrations of Composite Bars by BEM*", Composite Structures, Vol. 70, pp. 229-239, 2005.

[29] Sapountzakis E. J., "*Torsional Vibrations of Composite Bars of Variable Cross-Section by BEM*", Computational Methods and Applied Mechanical Engineering, Vol. 194, pp. 2127-2145, 2005.

[30] Cheong S.K., Kang K.W. and Jeong S.K., "*Evaluation of the Mechanical Performance of Golf Shafts*", Engineering Failure Analysis, 2005.

[31] Gu Jian-Xin and Chan Siu-Lai, "*A Refined Finite Element Formulation for Flexural and Torsional Buckling of Beam-Columns with Finite Rotations*", Engineering Structures, Vol. 27, pp. 749-759, 2005.

[32] Troyani N., Perez A. and Baiz P. *"Effect of Finite Element Mesh Orientation on Solution Accuracy for Torsional Problems*" Finite Elements in Analysis and Design, Vol 41, pp. 1377–1383, 2005